Research Square

Preprints are preliminary reports that have not undergone peer review.
They should not be considered conclusive, used to inform clinical practice,
or referenced by the media as validated information.

Identification of a Repressor for the Two *iol* Operons Required for Inositol Catabolism in Geobacillus Kaustophilus

Ken-ichi Yoshida (kenyoshi@kobe-u.ac.jp)
Kobe University https://orcid.org/0000-0002-3383-4664
Yusuke Shirae
Kobe Daigaku
Ryo Nishimura
Kobe Daigaku
Kaho Fukui
Kobe Daigaku
Shu Ishikawa
Kobe Daigaku

Research article

Keywords: Geobacillus, Gram-positive, thermophile, repressor, inositol

Posted Date: June 17th, 2020

DOI: https://doi.org/10.21203/rs.3.rs-35185/v1

License: This work is licensed under a Creative Commons Attribution 4.0 International License.
Read Full License

Version of Record: A version of this preprint was published at Microbiology on January 1st, 2021. See the published version at https://doi.org/10.1099/mic.0.001008.

Abstract

Background

Geobacillus kaustophilus HTA426, a thermophilic Gram-positive bacterium, grows on inositol as its sole carbon source, and an *iol* gene cluster required for inositol catabolism has been postulated with reference to the *iol* genes in *Bacillus subtilis*. The *iol* gene cluster consists of two tandem operons induced in the presence of inositol; however, the mechanism underlying the induction remains unclear. *B. subtilis iolQ* is known to be involved in the regulation of *iolX* encoding a *scyllo*-inositol dehydrogenase, and its homolog in HTA426 was found two genes upstream of the first gene (*gk1899*) of the *iol* gene cluster and termed as *iolQ* in *G. kaustophilus*.

Results

When *iolQ* was inactivated, not only the *myo*-inositol dehydrogenase activity in the cell due to the expression of *gk1899* but also the transcription of the two *iol* operons became constitutive. IolQ was produced and purified as a C-terminal His-tag fusion in *Escherichia coli* and subjected to the in vitro gel mobility shift assay to examine its DNA binding property. It was observed that IolQ bound to the DNA fragments containing each of the two *iol* promoter regions, and its DNA binding was antagonized by *myo*-inositol. Moreover, DNase I footprint analyses were conducted to determine the two binding sites of IolQ within each of the *iol* promoter regions. By comparing the sequences of the binding sites, a consensus sequence for IolQ binding was deduced to be a palindrome of 5'-RGWAAGCGCTTSCY-3' (where R = A or G, W = A or T, S = G or C, and Y = C or T).

Conclusion

IolQ functions as a transcriptional repressor regulating the induction of the two *iol* operons responding to *myo*-inositol.

Background

There is extensive research on the biochemical pathway and the regulation of bacterial inositol catabolism in *Bacillus subtilis*. It has been reported that *B. subtilis* possesses a complete set of *iol* genes required for its inositol catabolism; including the *iolABCDEFGHIJ* operon, the *iolRS* operon, *iolQ*, *iolT*, *iolU*, *iolW*, and *iolX* [1, 2, 3, 4, 5, 6].

The *iolABCDEFGHIJ* operon encodes the enzymes responsible for the primary pathway of inositol catabolism [7, 8], whereas *iolT* was found to encode the major inositol transporter [4]. A repressor encoded by *iolR* is the major transcription factor that belongs to the DeoR family and regulates the transcription of the *iolABCDEFGHIJ* operon and *iolT* [2, 4]. In the absence of inositol in the culture medium, the IolR repressor binds to the respective promoter regions to arrest the initiation of transcription. However, in the presence of inositol, one of the metabolic intermediates appearing in the

catabolic pathway, 2-deoxy-d-glucuronic acid 6-phosphate produced in the IolC reaction, acts as an inducer in vivo to antagonize the repressor function of IolR, leading to the transcriptional induction of the *iolABCDEFGHIJ* operon and *iolT* [1, 2, 4]. The process of regulation of *iol* genes by IolR homologs could be conserved among a number of bacterial species, including Gram-negative bacteria. For instance, *Sinorhizobium meliloti* belonging to Alphaproteobacteria, was shown to possess the *iol* genes regulated by its IolR ortholog [9], and in *Salmonella enterica*, belonging to Gammaproteobacteria, its IolR ortholog was found to regulate not only the transcription of *iol* genes [10] but also an orphan regulator encoded by *reiD* involved in *myo*-inositol utilization [11].

On the other hand, a recent study demonstrated that in *B. subtilis*, an additional repressor encoded by *iolQ* that belongs to the LacI family regulates *iolX*, encoding an NAD^+-dependent *scyllo*-inositol dehydrogenase [3], although the mechanisms underlying the regulation of *iolU* and *iolW*, either of which encodes an $NADP^+$-dependent *scyllo*-inositol dehydrogenase [5, 6], have not been elucidated as they appeared to be almost constitutive. Genetic evidence suggests that *scyllo*-inositol and *myo*-inositol could be the intracellular inducers for IolQ; however, both failed to antagonize its DNA binding activity in vitro [3].

Geobacillus kaustophilus HTA426 is a Gram-positive, thermophilic, and facultative anaerobic bacterium isolated from the deep-sea sediment collected from the Mariana trench in the western Pacific Ocean [12, 13]. It can grow at higher temperatures from 48 °C to 74 °C, optimally at 60 °C [13]. Its entire genome was sequenced [13], and some methodologies for its genetic manipulation have also been established [14, 15, 16]. Furthermore, this bacterium was found to possess a gene cluster with a composition similar to the complete set of *iol* genes elucidated in *B. subtilis* [17] (Fig. 1). In fact, it has been demonstrated that *G. kaustophilus* metabolizes at least three inositol stereoisomers, including *myo*-inositol, *scyllo*-inositol, and d-*chiro*-inositol [17]. In the *G. kaustophilus* genome, the *iol* gene cluster is separated into two operons; the first operon is 5-kb long containing 4 genes of *gk1896–1899*, and the second one is 12-kb long containing 10 genes of *gk1885–1894*, both of which are induced in parallel in the presence of inositol [17]. However, till date, no experimental study has been conducted to elucidate how these two operons are regulated for their induction.

Therefore, in the present study, we focused on the *gk1901*gene of *G. kaustophilus* homologous to the *iolQ* gene of *B. subtilis*, which is presumed to be a repressor belonging to the LacI family and located close upstream of the *iol* gene cluster (Fig. 1). We explored the function of *gk1901*, renamed here as *iolQ* in *G. kaustophilus*, encoding a repressor that bound to the two promoter regions within the *iol* gene cluster and was responsible for their transcriptional induction in the presence of *myo*-inositol.

Results

Inactivation of IolQ (gk1901) rendered myo-inositol dehydrogenase constitutive

In *B. subtilis*, *iolR* encodes the major transcription regulator (repressor) for the *iolABCDEFGHIJ* operon and *iolT* [1, 2, 4]. We attempted to identify a counterpart of *iolR* within the genome of *G. kaustophilus* HTA426 using the conventional homology search tool BLASTP [18]. The best candidate was found to be *gk1840*, which is predicted to encode a transcriptional regulator, belonging to the DeoR family, annotated as a fructose operon transcriptional repressor, and sharing a homology with *iolR* [Bit-score = 102 bits (253); E-value = 1e-26]. In contrast, a recent study showed that *B. subtilis iolX* is regulated by another repressor encoded by *iolQ* [3]. The best candidate for an *iolQ* counterpart in *G. kaustophilus* was *gk1901*, which encodes a transcriptional regulator of the LacI family and shares a much higher homology with *B. subtilis iolQ* [Bit-Score = 353 bits (905); E-value = 5e-121]. Furthermore, *gk1901* was located close (only two genes upstream) to the first gene of the *iol* gene cluster (*gk1899*). Therefore, we focused on *gk1901* as the possible candidate for the regulator of the *iol* genes in *G. kaustophilus* and created a mutant strain YS202, in which the entire coding region of *gk1901* was deleted by replacement with a kanamycin-resistant gene (Table 1).

Table 1
Bacterial strains and plasmids used in this study.

Strain or plasmid	Description and relevant properties	Source or reference
Geobacillus kaustophilus		
HTA426	Wild-type	[13]
MK72	Δ*pyrF* Δ*pyrR*	[15]
YS202	Δ*iolQ* Δ*pyrF* Δ*pyrR*	This work
Escherichia coli		
BL21(DE3)	F^- *ompT hsdSB*(rB^- mB^-) *gal*(λ*cI857 ind1 Sam7 nin5 lacUV5-T7gene1*) *dcm*(DE3)	Takara Bio
BR408	Donor strain for conjugative plasmid transfer	[15]
DH5α	F^- Φ80d *lacZ*Δ*M15* Δ(*lacZYA-argF*)U169, *deoR recA1 endA1 hsdR17*(rK^- mK^+) *phoA supE44* λ^- *thi-1 gyrA96 relA1*	Takara Bio
Plasmid		
pET30a(+)	*kan*	Takara Bio
pETiolQhisGK	*kan* P*t7-iolQ-his*	This work
pGKE24	*oriT pyrF amp*	[39]
pGKEdiolQ	A derivative of pGKE25	This work
pMD20	amp	Takara Bio

It is known that the NAD^+-dependent *myo*-inositol dehydrogenase is encoded by *gk1899*, which is the first gene of the *iol* gene cluster and transcribed from a promoter located its own upstream to be induced in the presence of inositol in the growth medium [17]. In the parental strain MK72 (a derivative of HTA426 lacking both functional *pyrF* and *pyrR*, which had previously been constructed for the counter selection system [15]) grown in the minimal medium containing 0.1% casamino acids as the carbon source supplemented with and without 10 mM *myo*-inositol, the activity of NAD^+-dependent *myo*-inositol dehydrogenase was repressed in the absence of *myo*-inositol but induced in its presence; in contrast, the activity became completely constitutive in YS202 lacking *gk1901* (Table 2). These results suggested that *gk1901* is involved in the induction mechanism of the *iol* genes, including *gk1899*. Consequently, we renamed *gk1901* as *iolQ* of *G. kaustophilus* hereafter.

Table 2

NAD^+-dependent *myo*-inositol dehydrogenase activity in strains of *G. kaustophilus*.

Strain	**NAD^+-dependent *myo*-inositol dehydrogenase activity (nmol/min/mg protein)**								
	None*			***myo*-Inositol***			***myo*-Inositol + Glucose***		
MK72	10.6	±	4.3	287.2	±	13.0	256.4	±	31.7
YS202	357.9	±	39.5	400.5	±	26.8	377.8	±	11.7

*Bacterial strains were grown in the liquid minimal medium containing both 0.1 g/ml casamino acids and 1 μg/ml uracil and additionally supplemented with the carbon sources as indicated (each 10 mM). Values are mean ± SD of three independent measurements.

On the other hand, the enzyme activities that were induced in MK72 and constitutive in YS202 were not repressed in the presence of additional glucose in the medium (Table 2), a finding that was consistent with the previous report that the *iol* genes in *G. kaustophilus* were not under catabolite repression [17].

iolQ encodes a regulator involved in the transcriptional induction of the two iol operons of G. kaustophilus

The constitutive activity of the NAD^+-dependent *myo*-inositol dehydrogenase in YS202 lacking *iolQ* suggested that the transcription of the *iol* genes in *G. kaustophilus* is regulated by *iolQ*. YS202 and its parental strain MK72 were grown in the presence and absence of *myo*-inositol, and their total RNAs were extracted and then subjected to northern blot analyses (Fig. 2). The internal short stretches of the coding regions of *gk1899* and *gk1894* were used as probes to detect the transcripts of 5- and 12-kb operons [17], respectively. In MK72, as previously found in HTA426, the specific transcripts of the two operons were detected only in the presence of *myo*-inositol [17], whereas in YS202, both were completely constitutive irrespective of the presence or absence of *myo*-inositol (Fig. 2). Our results clearly indicated that *iolQ* was involved in the transcriptional regulation, especially induction responding to *myo*-inositol, of the two *iol* operons.

IolQ bound to DNA fragments containing each of the two iol promoter regions in vitro

The northern blot analyses showed that *iolQ* was involved in the repression of the two operons of *iol* genes in the absence of *myo*-inositol. Therefore, we examined whether IolQ could bind to the promoter regions of the two *iol* operons. For this purpose, *iolQ* was cloned into pET30a(+) to be expressed as a C-terminal His-tag fusion (*IolQ-his*) and purified in *Escherichia coli* BL21(DE3). The production and purification of IolQ-his (approximately 35 kDa) were confirmed (Fig. 3), after which IolQ-his was subjected to gel mobility shift analyses to check whether it binds to the upstream sequences of the two *iol* operons in vitro as follows.

The transcriptional start point of the former 5-kb-long operon containing *gk1896–1899* was previously defined at 136-bp upstream from the start codon of *gk1899* [17], and the corresponding − 35 and − 10 regions were deduced to be the P*gk1899* region (Fig. 4A). To determine the transcriptional start point of the latter 12-kb-long operon for *gk1885–1894*, we conducted a 5'-rapid amplification of cDNA ends (5'-RACE) analysis using the total RNA sample prepared from the strain MK72 grown in the presence of *myo*-inositol (Fig. 2). Based on the results, we could identify a transcriptional start point at 210-bp upstream from the start codon of *gk1894* (Fig. 4B), and the corresponding − 35 and − 10 regions were found to be the P*gk1894* region.

For gel mobility shift analyses, the following three DNA fragments were prepared: the P*gk1894* fragment containing the stretch from − 400 to − 100 of the *gk1894* start codon, the P*gk1899* fragment containing the stretch from − 250 to + 50 of the *gk1899* start codon, and the negative control fragment corresponding an internal coding sequence of *gk1894* containing + 959 to + 1109 from the start codon. A fixed amount of DNA fragments was reacted with increasing concentrations of IolQ-his in vitro and loaded onto the polyacrylamide gel. Both the P*gk1894* and *Pgk1899* fragments exhibited an obvious gel mobility shift, forming DNA–protein complexes in a dose-dependent manner with the increase in the concentration of IolQ-his, whereas the negative control fragment did not exhibit such a result (Fig. 5). On the other hand, when one of *myo*-inositol, *scyllo*-inositol, *scyllo*-inosose, and ribose was added to the DNA–protein reaction mixture, the gel mobility shifts of the P*gk1894* and *Pgk1899* fragments were reduced partially but significantly only in the presence of *myo*-inositol (Fig. 5). These results indicated that IolQ-his bound to each of the P*gk1894* and *Pgk1899* fragments specifically and that *myo*-inositol could antagonize the interaction between each of the DNA fragments and IolQ-his.

Two IolQ binding sites within each of the iol promoter regions

All the above-described results suggested that IolQ could be a transcriptional repressor of the two *iol* operons that are induced in the presence of *myo*-inositol. We conducted DNase I footprint analyses to define the IolQ binding sites within the two promoter regions. The DNA fragments corresponding to each of the promoter regions were prepared using the respective 5'-6-carboxyfluorescein (6-FAM)-labeled primers and reacted with IolQ-his under the conditions similar to those used in the gel mobility shift analyses. The DNA–protein complexes were treated with DNase I, and the digested DNA was subjected to fragment size analysis to determine the regions protected from DNase I by the bound IolQ-his (Fig. 6). The results suggested that there could be two protected regions within each of the two *iol* promoter

regions (Figs. 4 and 6, the nucleotide sequences of upper and lower strands of the protected regions are shown in red), although the protection in the lower strand of the P*gk1894* fragment was less evident than that in the others due to unknown reason (Fig. 6D). The protected regions could be considered as the IolQ binding sites, and a comparison of the nucleotide sequences among the four binding sites allowed us to deduce a conserved palindromic sequence of 5'-RGWAAGCGCTTSCY-3' (where R = A or G, W = A or T, K = G or C, and Y = C or T) recognized by IolQ.

Each of the two *iol* promoter regions contained two IolQ binding sites, and four additional DNA fragments were prepared to contain each one of the IolQ binding sites as follows: for the P*gk1899* region, fragment A1, containing the stretch from − 250 to − 50 of the *gk1899* start codon, and fragment A2, from − 108 to + 114, whereas for the P*gk1894* region, fragment B1, containing the stretch from − 460 to − 284 of the *gk1894* start codon, and fragment B2, from − 304 to − 100 (Fig. 7). The four fragments were subjected to another set of gel mobility shift assays to confirm whether IolQ bound to any of them, although fragment A2 failed to form a clear protein–DNA complex (Fig. 7). For either promoter region, it was suggested that IolQ exhibited higher affinities to the binding sites adjacent to the respective transcriptional start points, contained in fragments A1 and B2, than to the other binding sites in fragments A2 and B1. In addition, *myo*-inositol could antagonize the binding of IolQ to all fragments.

Discussion

The majority of genes involved in inositol catabolism in bacterial systems have been demonstrated under the regulation of the repressor IolR belonging to DeoR family [1, 2, 4, 9, 10]. However, in *B. subtilis*, a recent research showed that the LacI family transcriptional repressor IolQ regulates the gene *iolX* for *scyllo*-inositol dehydrogenase [3]. Therefore, we focused on the *iolQ* gene of *G. kaustophilus* (a homolog of *iolQ* of *B. subtilis*, designated formerly as *gk1901* in databases), which is located two genes upstream of the *iol* gene cluster comprising two operons; the first operon is 5-kb long containing 4 genes of *gk1896-1899*, and the second one is 12-kb long containing 10 genes of *gk1885-1894*, as we speculated that *iolQ* might be involved in the transcriptional regulation of the two *iol* operons. The NAD^+-dependent *myo*-inositol dehydrogenase encoded by *gk1899* (the first gene of the former 5-kb-long *iol* operon) is known to be induced only in the presence of inositol in the culture medium [17]. We observed that the inactivation of *iolQ* rendered not only the NAD^+-dependent *myo*-inositol dehydrogenase (Table 2) but also the transcription of the two *iol* operons constitutive (Fig. 2). Furthermore, the gel mobility shift analyses revealed that IolQ bound to the promoter regions of both the *iol* operons, and its DNA binding activity was antagonized in the presence of *myo*-inositol (Fig. 5). All these results indicated that in *G. kaustophilus*, *iolQ* encoded a transcriptional repressor regulating the induction of the two *iol* operons responding to *myo*-inositol.

G. kaustophilus can grow not only on *myo*-inositol but also on other inositol stereoisomers, including *scyllo*-inositol and d-*chiro*-inositol [17], suggesting that these inositol isomers would also induce the *iol* operons. In *B. subtilis*, *iolW* and *iolI*, which are the respective homologs of *gk1898* and *iolI* of *G. kaustophilus*, are required to metabolize *scyllo*-inositol and d-*chiro*-inositol, respectively [19, 20] (Fig. 1).

Moreover, studies have shown that these genes together with *iolG*, the counterpart of *gk1899* of *G. kaustophilus*, are also involved in interconversion among *myo*-inositol, *scyllo*-inositol, and d-*chiro*-inositol [19, 20]. In the present study, we demonstrated that the two *iol* operons of *G. kaustophilus* are under the regulation of IolQ and that the DNA binding activity of IolQ was antagonized exclusively by *myo*-inositol in vitro. In *G. kaustophilus*, *gk1898* and *gk1899* are contained in the former 5-kb operon, whereas *iolI* is the third gene of the latter 12-kb operon. The transcriptional repression by IolQ might allow some basal expression of *iol* genes (Table 2), and this may allow *gk1898*, *iolI*, and *gk1899* to function to convert *scyllo*-inositol and d-*chiro*-inositol into *myo*-inositol in the cell to induce the *iol* operons. On the other hand, the inositol transporters in *G. kaustophilus* have not been identified yet; however, some genes included in the two *iol* operons, such as *gk1893*, *1894*, and *1895* possibly composing an ABC transporter and *gk1885* encoding a member of the major facilitator superfamily [13], might serve as *myo*-inositol transporter(s) with broader specificity to uptake any of these inositol isomers. The broader specificity in the inositol transporters was reported for that in *Caulobacter crescentus* that transports not only *myo*-inositol but also ribose [21]. Although ribose might be an additional substrate of the putative inositol transporters, it is unlikely that ribose acts an inducer in *G. kaustophilus* because the gel mobility shift assays showed that IolQ binding to the DNA fragments of the *iol* promoter regions was not antagonized by ribose (Fig. 5), and to our knowledge, there is no report describing any pathway involved in converting ribose into *myo*-inositol.

The transcription of *iol* genes in a number of bacterial species, including *B. subtilis*, *Clostridium perfringens*, *Lactobacillus casei*, *Salmonella enterica*, and *Sinorhizobium meliloti*, is repressed in the presence of glucose and thus under carbon catabolic repression [10, 22, 23, 24, 25, 26]. Catabolite repression in Gram-positive bacteria such as *B. subtilis* involves transcriptional repression through CcpA/P-Ser-HPr binding to the specific chromosomal sites with *cre* sequence [26]. As *gk2810* was identified within the *G. kaustophilus* genome to be highly homologous to the *ccpA* gene of *B. subtilis*, it was considered that the carbon catabolite repression might function in *G. kaustophilus* in a similar manner as that in *B. subtilis.* However, the *iol* genes in *G. kaustophilus* were not subjected to catabolite repression at all (Table 2) [17]. This finding implied that the inositol catabolism in *G. kaustophilus* might have a physiological significance other than being a simple strategy to utilize this carbon source, and a similar finding has been discussed with respect to another Gram-positive bacterium, *Corynebacterium glutamicum* [27, 28]. As already mentioned, *G. kaustophilus* HTA426 was isolated from the deep-sea sediment collected from the Mariana trench in the western Pacific Ocean [12, 13]. It has been reported that inositols are often found on the deep seafloor [29] and could be considered as osmotic regulators (osmolytes) [30, 31]. Deep-sea organisms are known to accumulate osmolytes to increase their intracellular osmotic pressure to adapt to the specific environment in the deep-sea [32]. Moreover, *scyllo*-inositol is particularly known as a chemical chaperone that interferes in the aggregation of denatured proteins such as amyloid beta accumulating in the brain resulting in the development of Alzheimer's disease [33, 34]. Through the possible interconversion among inositol stereoisomers [17, 20], some *scyllo*-inositol might be produced in *G. kaustophilus* to prevent the aggregation of proteins denatured under lower temperatures and high pressure in the deep-sea. The *iol* genes in *G. kaustophilus* might have been

excluded from the general control of carbon catabolite repression to be responsible for such a specific cellular function.

Each of the two *iol* promoter regions (P*gk1899* and P*gk1894*) had a pair of IolQ binding sites that were found to share a palindromic consensus sequence of 5'-RGWAAGCGCTTSCY-3' (Fig. 5). Within the genome sequence of *G. kaustophilus*, the consensus sequence can be found in the intergenic regions preceding *gk0016* (a hypothetical protein), *gk0786* (a transposase), *gk1017* (a hypothetical protein), *gk2450* (a 50S ribosomal protein L33), *gk2733* (a hypothetical protein), and *gk3430* (a glycyl-tRNA synthetase) [13]. IolQ might have the ability to bind to these sites, as IolQ-his could bind to the DNA fragments containing only one of the binding sites of the *iol* promoter regions (Fig. 7). However, the presence of pairwise IolQ binding sites is specific to the two *iol* promoter regions, suggesting that the closely located two binding sites are required to establish the transcriptional repression via IolQ binding. In fact, IolQ belongs to the transcription factors of the LacI family, which is represented by LacI of *E. coli* forming a dimeric structure to bind to the two operator sites of the lactose operon [35], and the two DNA-bound LacI dimers associate into a tetramer to form a DNA loop structure [36]. It has been observed that RNA polymerase cannot bind to the looped-out promoter due to steric hindrance, resulting in tighter repression [37]. Results of our DNase I footprint analyses revealed that the DNA containing the P*gk1899* region was not looped-out via IolQ binding, whereas that containing the P*gk1894* region could be (Fig. 5). In fact, it has been observed that the transcription driven by P*gk1899* is less tightly repressed in the absence of *myo*-inositol than that driven by P*gk1894* [38].

In *B. subtilis*, IolQ was found to act as a transcriptional repressor of *iolX*, encoding the NAD^+-dependent *scyllo*-inositol dehydrogenase [5]. *B. subtilis* IolQ binds to the two sites with a consensus sequence of 5'-AGAAARCGCTTKCKCAAA-3' (where K = G or T) in the *iolX* promoter region [5]. *scyllo*-Inositol and *myo*-inositol might possibly be the intracellular inducers; however, neither of them antagonized its DNA binding activity in vitro [5]. In contrast, in our study, we have clearly demonstrated that *G. kaustophilus* IolQ bound to the four binding sites with a palindromic consensus sequence of 5'-RGWAAGCGCTTSCY-3' and its DNA binding activity was antagonized by *myo*-inositol. These two repressor proteins share a certain similarity in their amino acid sequences and the consensus sequences required for their binding, and in addition, both are functionally related based on their involvement in the regulation of the genes required for inositol catabolism. Further investigation of the similarities and differences between the two IolQs may yield some implications for understanding the evolution of the regulatory genes with related functions.

Conclusions

The *iolQ* gene of *G. kaustophilus* (formerly known as *gk1901*) is located two genes upstream of the *iol* gene cluster comprising two tandem operons. The NAD^+-dependent *myo*-inositol dehydrogenase encoded by *gk1899* (the first gene of the *iol* cluster) is known to be induced only in the presence of inositol in the culture medium. Our results showed that the inactivation of *iolQ* rendered not only the NAD^+-dependent *myo*-inositol dehydrogenase but also the transcription of the two *iol* operons constitutive. Furthermore,

the gel mobility shift analyses demonstrated that IolQ bound to the promoter regions of both the *iol* operons and its DNA binding activity was antagonized in the presence of *myo*-inositol. All these results indicated that in *G. kaustophilus*, *iolQ* encoded a transcriptional repressor regulating the induction of the two *iol* operons responding to *myo*-inositol. We also conducted DNase I footprint analyses to determine the two binding sites of IolQ within each of the *iol* promoter regions. By comparing the sequences of the binding sites, we deduced that the consensus sequence required for IolQ binding was a palindrome of 5'-RGWAAGCGCTTSCY-3' (where R = A or G, W = A or T, S = G or C, and Y = C or T).

Methods

Bacterial strains, plasmids, primers, and growth conditions

The strains and plasmids used in this study are shown in Table 1, and the primers are depicted in Table 3. Strains of *E. coli* cultures were grown aerobically at 37 °C in LB medium containing 25 μg/ml ampicillin or 25 μg/ml kanamycin as needed. Strains of *G. kaustophilus* were grown aerobically at 60 °C in LB medium or minimal medium containing 1.72 mM K_2SO_4, 1.39 μM $ZnSO_4$, 162 nM H_3BO_3, 238 nM $CoCl_2$, 800 nM $CuSO_4$, 42 nM $NiCl_2$, 744 nM EDTA-2Na, 2.79 mM Na_2HPO_4, 11.1 μM $MnCl_2$, 1.62 mM $MgSO_4$, 34.1 μM $CaCl_2$, 25.9 μM $FeCl_3$, 18.7 mM NH_4Cl, 10.0 mM K-MOPS (pH 8.0), and carbon sources (10 mM *myo*-inositol, 10 mM glucose, and 0.1% casamino acids). When required, 1 or 100 μg/ml uracil and 50 μg/ml 5-fluoroorotic acid (5-FOA) were added.

Table 3
Primers used in this study.

Primer	Sequence (5'-3')
gk1901-UF	GGAAACAGCTATGACAGGAAATAACATCGCTTTATG
gk1901-UR	TTATTTTTCGGTCGATCATCGCTCATCATTCTCTC
gk1901-DF	AAATCGTAAGGATGTGAGCA
gk1901-DR	GAATTCGTAATCATGGAACAGACCGAGGCCCGG
pGKE25-ER	AATTCACTGGCCGTCGTTTTAC
pGKE25-HF	AGCTTGGCGTAATCATGGTC
gk1901-F	AAGGAGATATACATAATGAAAGTAACCATTTACGATG
gk1901-R	GACGGAGCTCGAATTCGATTTCACTTTAGCGATATG
n-gk1894-F	CTATGTGCTGGAAATGATAGAC
n-gk1894-R	TAATACGACTCACTATAGGGGTTGCCTCGTCTTTTTGAC
n-gk1899-F	AGTAGGGATTTTGGGAGC
n-gk1899-R	TAATACGACTCACTATAGGGGTTTATACACCGACGCATACC
EMSA-UF	CCTTTTTCGACATAAGCC
EMSA-UR	ACCTTGGCAATCCCTCC
EMSA-DF	GGTTAGAGTAAGCGCTTGC
EMSA-DR	TAACAAAATTACCTTATTTAGCGC
EMSA-IF	GACGATCCGCTCGACGC
EMSA-IR	TGCAAAAAGCCTGCCTTC
EMSA-12UF	TGGCAGACGTTCATAAAATAG
EMSA-12UR	GCCTTATAACTGATCATTCATTG
EMSA-12DF	CAATGAATGATCAGTTATAAGGC
EMSA-5UR	ATCGAAAACAATGGTTATTATG
EMSA-5DF	GTTCGATGGAGATTAGATTG
EMSA-5DR	TTCCACAATATCCGCTACC
RT	CATGTTCGGAACAGGGC
S1	GGGAAATCGACATTGATG
S2	AAGAGTTGAAAGTCTCCACG

Primer	Sequence (5'-3')
A1	GAACCGTGCCTCTTTTAAC
A2	ACCGTCTAACGCTTTGAC

Construction Of Plasmids

pGKE25diolQ was prepared to construct the strain YS202 as described here. A 1.0-kb stretch corresponding to the upstream region of *iolQ* in the *G. kaustophilus* HTA426 chromosome was amplified by PCR using the primer pair of gk1901-UF/gk1901-UR (Table 3). Similarly, another 1.0-kb stretch corresponding to the downstream region of *iolQ* was amplified using gk1901-DF/gk1901-DR (Table 3). pGKE25 [39] was linearized by inverse PCR using pGKE25-ER and pGKE25-HF as primers (Table 3). The PCR fragments of the upstream and downstream regions of *iolQ* and the linearized pGKE25 were incubated with Gibson Assembly Master Mix (New England Bio) at 50 °C for 15 min and transformed into *E. coli* DH5α (Table 1) to yield the recombinant plasmid pGKE25diolQ, whose accurate construction was confirmed by DNA sequencing.

pETiolQhisGK was constructed as described subsequently, which was designed to express *IolQ-his* and purify the gene product as a C-terminal His-tag fusion in *E. coli*. The coding region of *iolQ* was amplified by PCR from the chromosome of HTA426 using the primer pair of gk1901-F/gk1901-R (Table 3). The PCR fragment and the DNA of pET30a(+) previously cleaved using NdeI and EcoRI were mixed and incubated for 15 min at 50 °C with Gibson Assembly Master Mix to produce pETiolQhisGK, whose accurate construction was confirmed by DNA sequencing.

Construction Of Strains

G. kaustophilus YS202 is a derivative of MK72 [15], which was constructed to introduce an in-frame deletion of *iolQ* as described here. The recombinant plasmid pGKE25diolQ was introduced into *E. coli* BR408 (Table 1) and then transferred into MK72 by conjugation as described previously [15] to form colonies on the minimal plate medium containing 0.1% casamino acids and 1% glucose without uracil at 60 °C. One of the resulting uracil non-demanding transconjugants was proliferated once in LB medium at 60 °C, and an aliquot of the culture was inoculated and allowed to grow in the minimal medium containing 0.1% casamino acids, 1% glucose, 1 μg/ml uracil, and 50 μg/ml 5-FOA for 24 h. From this culture, colonies were formed on the minimal medium plates containing 0.1% casamino acids, 1% glucose, 1 μg/ml uracil, and 50 μg/ml 5-FOA, and one of them was selected as the strain YS202, whose accurate construction was confirmed by DNA sequencing.

Inositol Dehydrogenase Assay

Strains of *G. kaustophilus* were grown aerobically in the liquid minimal medium containing 0.1% casamino acids and 1 μg/ml uracil and additionally supplemented with or without 10 mM *myo*-inositol. The bacterial cells were harvested by centrifugation and washed once in a buffer prepared using 1 M NaCl and 50 mM Tris-HCl (pH 8.0). The cells were suspended in 100 μl of 100 mM Tris-HCl (pH 8.0) and transferred into a microtube containing 5 μl of 10 mg/ml lysozyme in 100 mM Tris-HCl (pH 8.0). The cells were incubated at 37 °C, after which they were disrupted completely by Bioruptor UCD-250 (Cosmo Bio, Tokyo, Japan). After centrifugation, the supernatant was stored as the enzyme solution. Next, the activity of the NAD^+-dependent *myo*-inositol dehydrogenase in the enzyme solution was measured spectrophotometrically as described previously [17].

Rna Sample Preparation

Strains of *G. kaustophilus* were grown aerobically in the liquid minimal medium containing 0.1% casamino acids and 1 μg/ml uracil and additionally supplemented with or without 10 mM *myo*-inositol. The bacterial cells were collected and disrupted to extract the total RNA as described previously [17].

Northern Blot Analysis

The RNA samples were subjected to northern blot analyses using DIG-labeled RNA probes specific for *gk1894* and *gk1899*, as described previously [3]. The RNA probes were prepared as follows: the DNA fragments corresponding to the part of the *gk1894*- and *gk1899*-coding regions were amplified by PCR using the DNA of the strain HTA426 as a template and the primer pairs of n-gk1894-F/n-1894-R and n-gk1899-F/n-1899-R, respectively (Table 3) to introduce a T7 RNA polymerase promoter sequence in the tail. The PCR product was used as the template for in vitro transcription using a DIG RNA labeling kit (SP6/T7) (Roche Diagnostics, Basel, Switzerland) to produce the DIG-labeled RNA probes. Cellular RNAs were separated by gel electrophoresis, transferred to a positively charged nylon membrane (Roche Diagnostics), hybridized using the DIG-labeled probes, and then detected using a DIG luminescence detection kit (Roche Diagnostics).

5'-RACE

5'-RACE was performed to identify a transcriptional start point using the 5'-Full RACE Core Set (Takara Bio, Kusatsu, Japan) according to the protocol provided by the supplier. Briefly, the first strand of cDNA was synthesized from the RNA sample prepared from the cells of MK72 grown in the liquid minimal medium containing 0.1% casamino acids, 1 μg/ml uracil, and 10 mM *myo*-inositol by reverse-transcription reaction using a 5'-end phosphorylated RT primer (Table 3) and then treated with RNase H to liberate the single-stranded cDNA. The single-stranded cDNA was cyclized by T4 RNA ligase and subjected to the two-step nested inverse PCR using two PCR pairs of A1/S1 and A2/S2 (Table 3) successively. The resulting PCR fragments were cloned into the T vector pMD20 (Takara Bio) and sequenced to identify the transcriptional start point.

Purification Of IolQ-his

E. coli BL21(DE3) carrying pETIolQhisGK was grown aerobically in LB liquid medium containing kanamycin, and then 1 mM IPTG was added to the growing culture to induce the expression of *IolQ-his*. Bacterial cells were harvested, suspended in a buffer prepared using 50 mM phosphate buffer (pH 8.0), 20% glycerol, and 0.5 M NaCl, and then disrupted completely by Bioruptor UCD-250 (Cosmo Bio). After centrifugation, the supernatant was subjected to histidine tag fusion protein purification using TALON®Metal affinity resins (Takara Bio) according to the supplier's instructions. The eluted fractions were subjected to SDS-PAGE, and the purity of IolQ-his was confirmed.

Gel Mobility Shift Assay

The gel mobility shift assay was performed fundamentally based on the protocol described previously [40]. DNA fragments were prepared by PCR amplification from the DNA of HTA426. For preparation of the P*gk1894* fragment, the primer pair of EMSA-DF/EMSA-DR was used; for the P*gk1899* fragment, the primer pair of EMSA-UF/EMSA-UR was used; and for the negative control fragment corresponding to an internal coding sequence of *gk1894*, the primer pair of EMSA-IF/EMSA-IR was used (Table 3). The P*gk1894* fragment was divided into fragments B1 and B2 to separate the two IolQ binding sites, and similarly, the P*gk1899* fragment was divided into fragments A1 and A2. To prepare the fragments A1, A2, B1, and B2, the primer pairs EMSA-UF/EMSA-5UR, EMSA-5DF/EMSA-5DR, EMSA-12UF/EMSA-12UR, and EMSA-12DF/EMSA-DR were used, respectively (Table 3). A fixed amount of the DNA fragments and various amounts of the purified IolQ-his were mixed in a binding buffer containing 20 mM Tris-HCl (pH 8), 100 mM KCl, 0.5 mM $MgCl_2$, 0.5 mM dithiothreitol, 0.005 mg/ml poly[d(I-C)], 0.05 mg/ml bovine serum albumin, and 0.05% polyethylene glycol in an ice bath and reacted at 37 °C for 20 min. The reaction mixture was subjected to 6% (or 12%) polyacrylamide gel electrophoresis in 40 mM Tris-acetate (pH 8)/2 mM EDTA. After the completion of electrophoresis, the gel was soaked in 0.1 μg/ml cybergreen for 30 min, and the DNA bands were detected by the Gel Doc XR + system (Bio-Rad, Hercules, CA).

Dnase I Footprint Analysis

DNase I footprint analysis was conducted essentially as described previously [3]. PCR procedures were used to amplify 5'-6-FAM-labeled DNA fragments containing the P*gk1899* region from the DNA of the strain HTA426 using the specific primers of [6-FAM]EMSA-UF/EMSA-UR and EMSA-UF/[6-FAM]EMSA-UR for labeling the sense and antisense strands, respectively (Table 3). Similarly, 5'-6-FAM-labeled DNA fragments containing the *Pgk1894* region were amplified using the specific primer pairs of [6-FAM]EMSA-12UF/EMSA-DR and EMSA-12UF/[6-FAM]EMSA-DR for labeling the sense and antisense strands, respectively (Table 3). Each differentially 5'-6-FAM-labeled DNA fragment was incubated with varying concentrations of IolQ-his and digested by DNase I to be analyzed using the ABI 3130xl Genetic Analyzer

with the ABI Gene Mapper Software Ver. 4.0 (Thermo Fisher Scientific, Waltham, MA) together with the corresponding DNA sequencing reactions.

List of abbreviations

5-FOA, 5-fluoroorotic acid

5'-RACE, 5'-rapid amplification of cDNA ends

6-FAM, 6-carboxyfluorescein

DIG, digoxigenin.

Abbreviations

5-FOA, 5-fluoroorotic acid

5'-RACE, 5'-rapid amplification of cDNA ends

6-FAM, 6-carboxyfluorescein

DIG, digoxigenin.

Declarations

Ethics approval and consent to participate

Not applicable.

Consent for publication

Not applicable.

Availability of data and materials

The datasets generated and/or analyzed during the current study are available from the corresponding author on reasonable request.

Competing interests

The authors declare that they have no competing interests.

Funding

This work was supported by the Ministry of Education, Culture, Sports, Science, and Technology, Japan, by KAKENHI (18H02128).

Authors' contributions

YS, RN, and KF conducted most of the experiments and analyzed the results under the supervision of KY and SI. KY conceived the idea for the project and wrote the final manuscript with SI. All authors read and approved the final manuscript.

Acknowledgments

The authors are thankful to Hirokazu Suzuki for providing pGKE24.

References

1. Yoshida K, Aoyama D, Ishio I, Shibayama T, Fujita Y. Organization and transcription of the myo-inositol operon, iol, of Bacillus subtilis. J Bacteriol. 1997;179:4591–8.
2. Yoshida K, Shibayama T, Aoyama D, Fujita Y. Interaction of a repressor and its binding sites for regulation of the Bacillus subtilis iol divergon. J Mol Biol. 1999;285:917–29.
3. Kang DM, Michon C, Morinaga T, Tanaka K, Takenaka S, Ishikawa S, et al. Bacillus subtilis IolQ (DegA) is a transcriptional repressor of iolX encoding NAD^+-dependent scyllo-inositol dehydrogenase. BMC Microbiol. 2017;17:154.
4. Yoshida K, Yamamoto Y, Omae K, Yamamoto M, Fujita Y. Identification of two myo-inositol transporter genes of Bacillus subtilis. J Bacteriol. 2002;184:983–91.
5. Kang DM, Tanaka K, Takenaka S, Ishikawa S, Yoshida K. Bacillus subtilis iolU encodes an additional $NADP^+$-dependent scyllo-inositol dehydrogenase. Biosci Biotechnol Biochem. 2017;81:1026–32.
6. Morinaga T, Ashida H, Yoshida K. Identification of two scyllo-inositol dehydrogenases in Bacillus subtilis. Microbiology. 2010;156:1538–46.
7. Yoshida K, Yamaguchi M, Ikeda H, Omae K, Tsurusaki K, Fujita Y. The fifth gene of the iol operon of Bacillus subtilis, iolE, encodes 2-keto-myo-inositol dehydratase. Microbiology. 2004;150:571–80.
8. Yoshida K, Yamaguchi M, Morinaga T, Kinehara M, Ikeuchi M, Ashida H, et al. myo-Inositol catabolism in Bacillus subtilis. J Biol Chem. 2008;283:10415–24.
9. Kohler PR, Choong EL, Rossbach S. The RpiR-like repressor IolR regulates inositol catabolism in Sinorhizobium meliloti. J Bacteriol. 2011;193:5155–63.
10. Kröger C, Fuchs TM. Characterization of the myo-inositol utilization island of Salmonella enterica serovar Typhimurium. J Bacteriol. 2009;191:545–54.
11. Rothhardt JE, Kröger C, Broadley SP, Fuchs TM. The orphan regulator ReiD of Salmonella enterica is essential for myo-inositol utilization. Mol Microbiol. 2014;94:700–12.
12. Takami H, Inoue A, Fuji F, Horikoshi K. Microbial flora in the deepest sea mud of the Mariana Trench. FEMS Microbiol Lett. 1997;152:279–85.
13. Takami H, Nishi S, Lu J, Shimamura S, Takaki Y. Genomic characterization of thermophilic Geobacillus species isolated from the deepest sea mud of the Mariana Trench. Extremophiles

2004;8:351-6.

14. Suzuki H, Yoshida K. Genetic transformation of Geobacillus kaustophilus HTA426 by conjugative transfer of host-mimicking plasmids. J Microbiol Biotechnol. 2012;22:1279–87.
15. Suzuki H, Murakami A, Yoshida K. Counterselection system for Geobacillus kaustophilus HTA426 through disruption of pyrF and pyrR. Appl Environ Microbiol. 2012;78:7376–83.
16. Miyano M, Tanaka K, Ishikawa S, Mori K, Miguel-Arribas A, Meijer WJJ, et al. A novel method for transforming the thermophilic bacterium Geobacillus kaustophilus. Microb Cell Fact. 2018;17:127.
17. Yoshida K, Sanbongi A, Murakami A, Suzuki H, Takenaka S, Takami H. Three inositol dehydrogenases involved in utilization and interconversion of inositol stereoisomers in athermophile, Geobacillus kaustophilus HTA426. Microbiology. 2012;158:1942–52.
18. Altschul SF, Madden TL, Schäffer AA, Zhang J, Zhang Z, Miller W, Lipman DJ. Gapped BLAST and PSI-BLAST: a new generation of protein database search programs. Nucleic Acids Res. 1997;25:3389–402.
19. Yoshida K, Yamaguchi M, Morinaga T, Ikeuchi M, Kinehara M, Ashida H. Genetic modification of Bacillus subtilis for production of D-chiro-inositol, an investigational drug candidate for treatment of type 2diabetes and polycystic ovary syndrome. Appl Environ Microbiol. 2006;72:1310–5.
20. Yamaoka M, Osawa S, Morinaga T, Takenaka S, Yoshida K. A cell factory of Bacillus subtilis engineered for the simple bioconversion of myo-inositol to scyllo-inositol, a potential therapeutic agent for Alzheimer's disease. Microb Cell Fact. 2011;10:69.
21. Herrou J, Crosson S. myo-Inositol and D-ribose ligand discrimination in an ABC periplasmic binding protein. J Bacteriol. 2013;195:2379–88.
22. Yoshida K, Kobayashi K, Miwa Y, Kang CM, Matsunaga M, Yamaguchi H, et al. Combined transcriptome and proteome analysis as apowerful approach to study genes under glucose repression in Bacillus subtilis. Nucleic Acids Res. 2001;29:683–92.
23. Kawsar HI, Ohtani K, Okumura K, Hayashi H, Shimizu T. Organization and transcriptional regulation of myo-inositol operon in Clostridium perfringens. FEMS Microbiol Lett. 2004;235:289–95.
24. Yebra MJ, Zúñiga M, Beaufils S, Pérez-Martínez G, Deutscher J, Monedero V. Identification of a gene cluster enabling Lactobacillus casei BL23 to utilize myo-inositol. Appl Environ Microbiol. 2007;73:3850–8.
25. Kohler PR, Zheng JY, Schoffers E, Rossbach S. Inositol catabolism, a key pathway in Sinorhizobium meliloti for competitive host nodulation. Appl Environ Microbiol. 2010;76:7972–80.
26. Fujita Y. Carbon catabolite control of the metabolic network in Bacillus subtilis. Biosci Biotechnol Biochem. 2009;732:45–59.
27. Krings E, Krumbach K, Bathe B, Kelle R, Wendisch VF, Sahm H, et al. Characterization of myo-inositol utilization by Corynebacterium glutamicum: the stimulon, identification of transporters, and influence on L-lysine formation. J Bacteriol. 2006;188:8054–61.

28. Lindner SN, Seibold GM, Henrich A, Kramer R, Wendisch VF. Phosphotransferase system-independent glucose utilization in Corynebacterium glutamicum by inositol permeases and glucokinases. Appl Environ Microbiol. 2011;77:3571–81.
29. White RH, Miller SL. Inositol isomers: occurrence in marine sediments. Science. 1976;193:885–6.
30. Yancey PH. Compatible and counteracting solutes: protecting cells from the Dead Sea to the deep sea. Sci Prog. 2004;87:1–24.
31. Yancey PH. Organic osmolytes as compatible, metabolic and counteracting cytoprotectants in high osmolarity and other stresses. J Exp Biol. 2005;208:2819–30.
32. Yancey PH. Water Stress, Osmolytes and proteins. Amer Zool. 2001;41:699–709.
33. Townsend M, Cleary JP, Mehta T, Hofmeister J, Lesne S, O'Hare E, et al. Orally available compound prevents deficits in memory caused by the Alzheimer amyloid-beta oligomers. Ann Neurol. 2006;60:668–76.
34. McLaurin J, Kierstead ME, Brown ME, Hawkes CA, Lambermon MH, Phinney AL, et al. Cyclohexanehexol inhibitors of Abeta aggregation prevent and reverse Alzheimer phenotype in amouse model. Nat Med. 2006;12:801–8.
35. Matthews KS, Nichols JC. Lactose repressor protein: Functional properties and structure. Prog Nucleic Acid Res Mol Biol. 1998;58:127–64.
36. Oehler S, Eismann ER, Krämer H, Müller-Hill B. The three operators of the lac operon cooperate in repression. EMBO J. 1990;9:973–9.
37. Swint-Kruse L, Matthews KS. Allostery in the LacI/GalR family: variations on a theme. Curr Opin Microbiol. 2009;12:129–37.
38. Suzuki H, Yoshida K, Ohshima T. Polysaccharide-degrading thermophiles generated by heterologous gene expression in Geobacillus kaustophilus HTA426. Appl Environ Microbiol. 2013;79:5151–8.
39. Suzuki H, Kobayashi J, Wada K, Furukawa M, Doi K. Thermoadaptation-directed enzyme evolution in an error-prone thermophile derived from Geobacillus kaustophilus HTA426. Appl Environ Microbiol. 2015;81:149–58.
40. Hamoen LW, Venema G, Kuipers OP. Controlling competence in Bacillus subtilis: shared use of regulators. Microbiology. 2003;149:9–17.

Figures

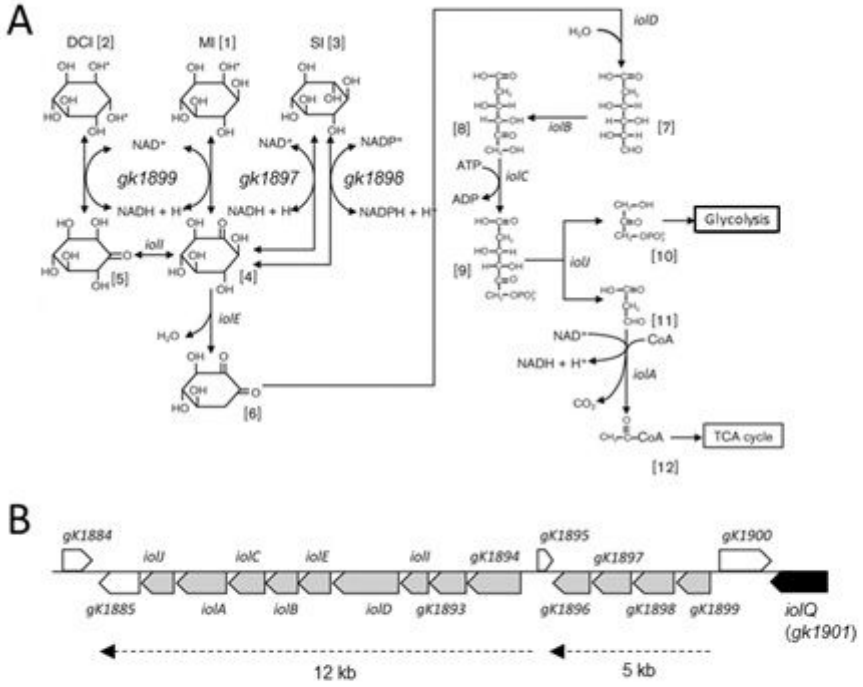

Yoshida *et al.*, Fig. 1

Figure 1

Predicted pathway of inositol catabolism (A) and schematic organization of the iol gene cluster in G. kaustophilus (B). Compounds: [1], myo-inositol; [2], D-chiro-inositol; [3], scyllo-inositol; [4], 2-keto-myo-inositol; [5], 1-keto-D-chiro-inositol; [6], (3,5/4)-trihydroxycyclohexane-1,2-dione; [7], 5-deoxy-D-glucuronic acid; [8], 2-deoxy-5-keto-D-gluconic acid; [9], 2-deoxy-5-keto-D-gluconic acid phosphate; [10], dihydroxyacetone phosphate; [11], malonic semialdehyde; and [12], acetyl-CoA. For the inositol isomers, axial hydroxyl groups are indicated by asterisks. G. kaustophilus genes encoding the respective enzymes either proven or predicted to be involved in the various reaction steps of the inositol catabolic pathway are shown.

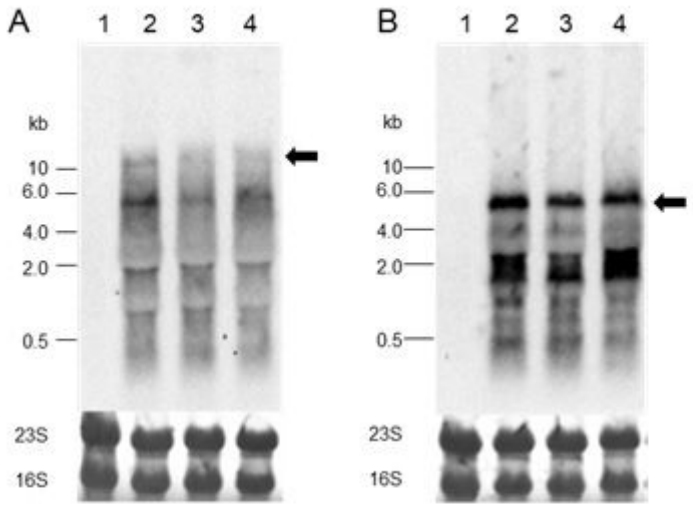

Yoshida *et al*., Fig. 2

Figure 2

Northern blot analyses of the two iol operons. Northern blot analyses for transcripts containing gk1899 (A) and gk1894 (B) were conducted using RNA samples prepared from cells of the strains MK72 (lanes 1 and 2) and YS202 (lanes 3 and 4) grown with (lanes 2 and 4) and without (lanes 1 and 3) 10 mM myo-inositol. Each of the lanes contained 20 μg of RNA samples. The 5- and 12-kb transcripts are indicated by arrowheads. Loading controls of rRNA (16S and 23S) are shown at the bottom.

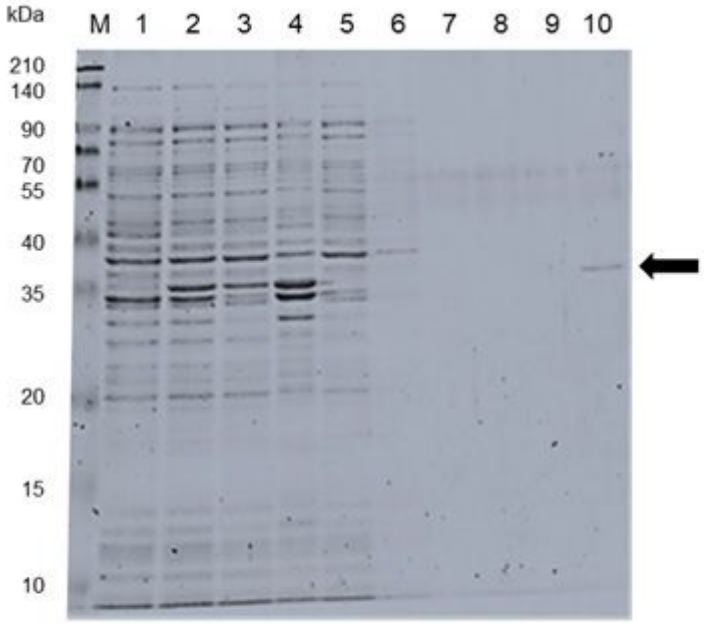

Yoshida *et al*., Fig. 3

Figure 3

Production and purification of IolQ-his. IolQ-his was produced and purified in E. coli by Ni-Co affinity chromatography and subjected to 12% SDS-polyacrylamide gel electrophoresis. Lane M, molecular weight markers; lane 1, whole cell grown without IPTG; lane 2, whole cell grown with 1 mM IPTG; lane 3, soluble fraction; lane 4, insoluble fraction; Lane 5, flow through fraction; lane 6, 1st wash fraction; lane 7, 2nd wash fraction; lanes 8–10, eluted fractions with stepwise increase of imidazole concentrations at 50, 100, and 200 mM, respectively. The arrowhead on the left side indicates the band of approximately 35 kDa protein corresponding to IolQ-his.

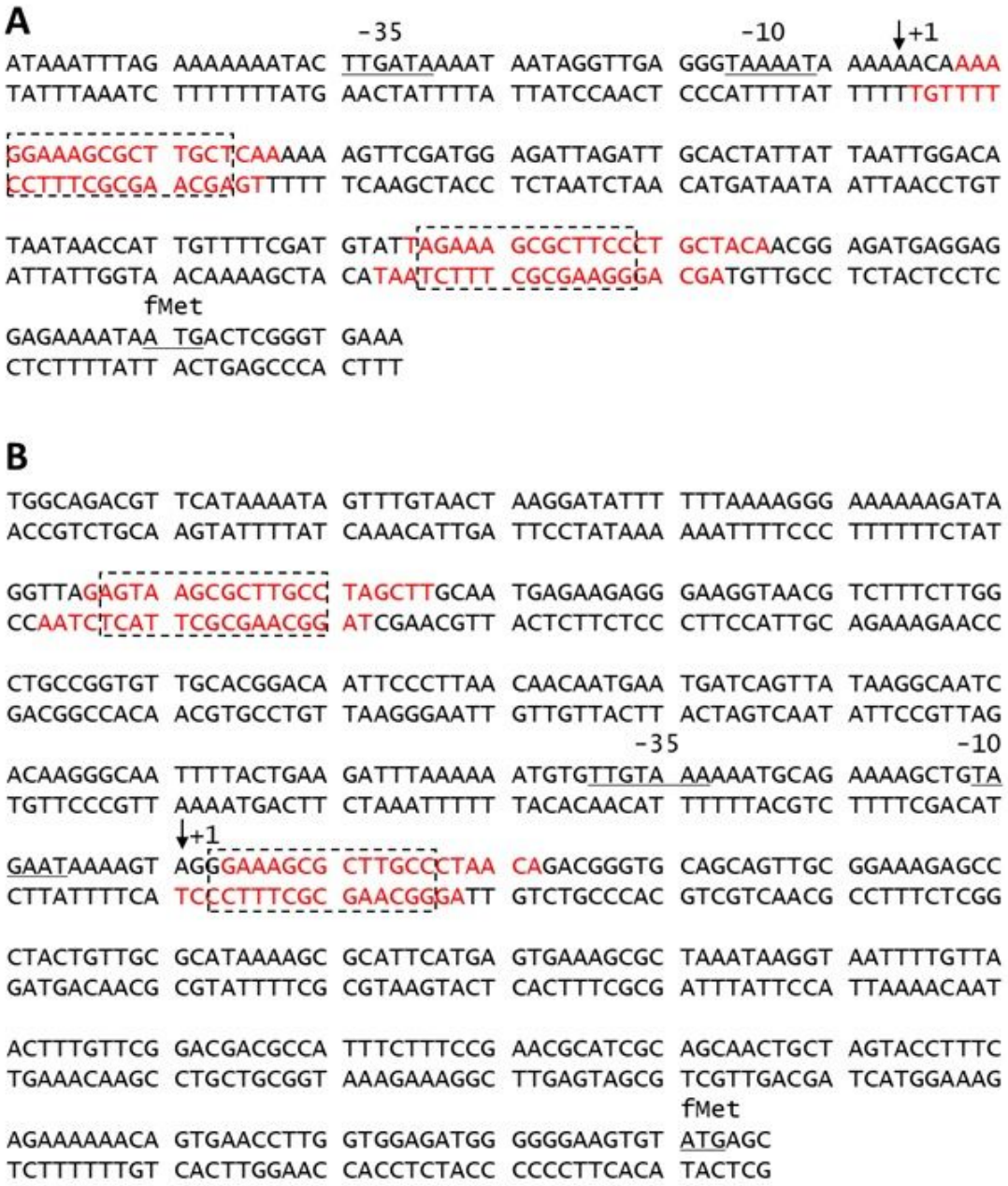

Yoshida *et al.*, Fig. 4

Figure 4

Nucleotide sequences of the two iol promoter regions (A, Pgk1899, and B, Pgk1894). The -35 and -10 regions, corresponding to transcriptional start points (+1) and translational start codons (fMet) are indicated in the upper strand. The nucleotides protected from DNase I by the bound IolQ-his are indicated in red letters in the sequence, and the region of consensus sequences are surrounded by dotted boxes.

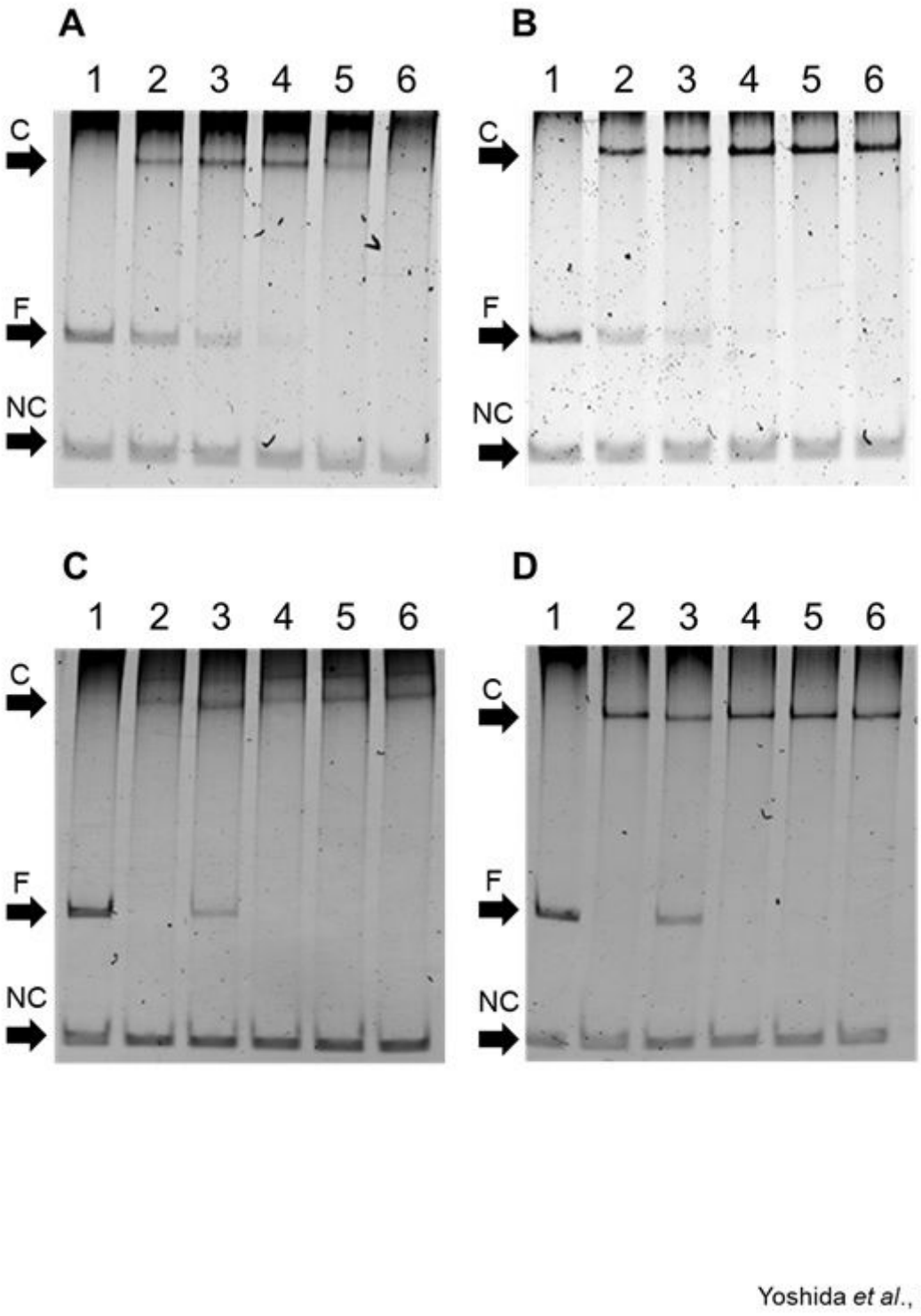

Yoshida *et al.*, Fig. 5

Figure 5

Gel mobility shift of DNA fragments containing the iol promoter regions caused by IolQ binding. The DNA fragment (2.3 nM) containing Pgk1894 (A) or Pgk1899 (B) was combined with the negative control fragment (2.3 nM) and incubated with various concentrations of IolQ-his (for lanes 1–6, 0, 5.7, 11.4, 22.8, 45.7, and 91.4 nM as monomer, respectively) and then subjected to 6% polyacrylamide gel electrophoresis. On the other hand, the DNA fragment (2.3 nM) containing Pgk1894 (C) or Pgk1899 (D) was combined with the negative control fragment (2.3 nM) and incubated without (lane 1) and with 91.4

nM IolQ-his (lanes 2–6) in the absence (lane 2) and the presence of one of the inducer candidate chemicals (lanes 3–6, myo-inositol, scyllo-inositol, scyllo-inosose, and ribose, respectively, each 1 mM). Positions of IolQ–DNA complex (C), free DNA (F), and negative control fragment (NC) are indicated by arrowheads.

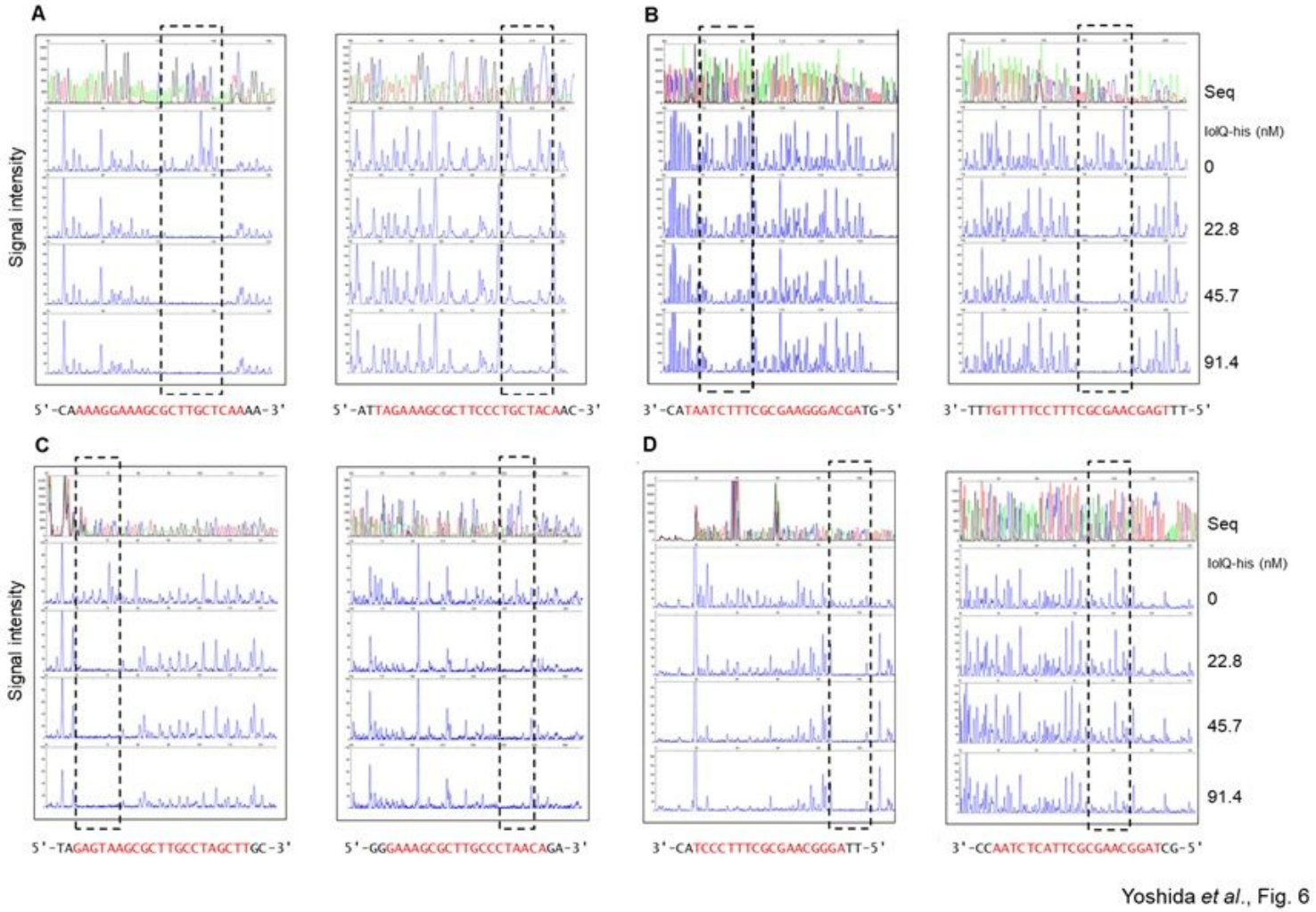

Figure 6

DNase I foot prints of IolQ on Pgk1899 (panels A and B) and Pgk1894 (C and D). For clarity, each of the panels has two sets of chromatograms, which are the two divisions of a continuous chromatogram; the left is the former part and the right is the latter. 2.3 nM of DNA fragments alternatively labeled with 6-FAM at the 5'-end of the upper (A and C) or lower strand (B and D) were reacted with IolQ-his and digested by DNase I before the fragment analysis performed as described in the main text. Each of the panels presents five chromatograms as follows: on the top, the sequencing chromatogram (Seq), and the second from the top to the fifth, the fragmentation patterns with various concentrations of IolQ-his (0, 22.8, 45.7, and 91.4 nM, respectively). The regions protected from DNase I by the bound IolQ-his are surrounded by dotted boxes and indicated as red letters in the nucleotide sequences beneath the respective chromatograms; for panels A and C, sequences of upper strands (5' to 3'), while for B and D, those of lower strands (3' to 5').

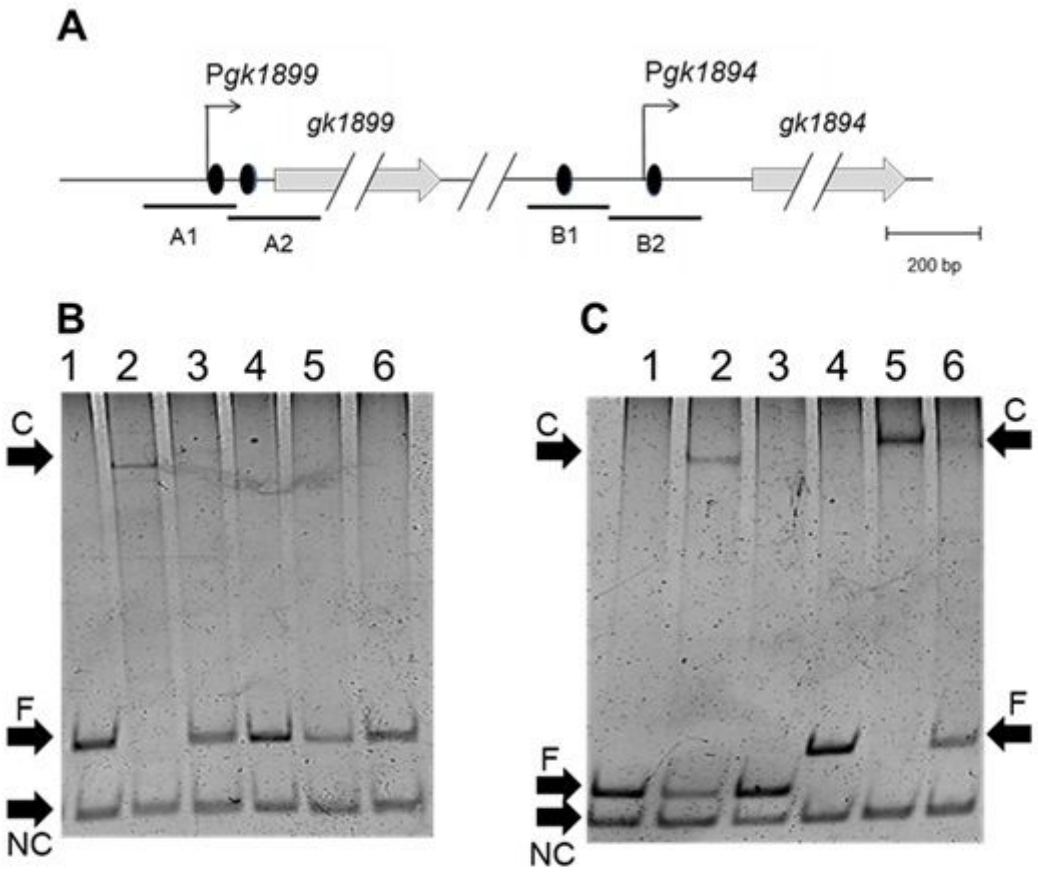

Yoshida *et al*., Fig. 7

Figure 7

Gel mobility shift of DNA fragments containing one of the tandem IolQ binding sites. Organization of the two iol promoter regions and positions of DNA fragments A1, A2, B1, and B2 relevant to the transcriptional start points (line arrows) and IolQ binding sites (ovals) (Panel A). Results of gel mobility shift assays for fragments A1 and A2 (panel B, lanes 1–3 and 4–6, respectively) and B1 and B2 (panel C, lanes 1–3 and 4–6, respectively). Each of the fragments (2.3 nM) was combined with the negative control fragment (2.3 nM), reacted without (lanes 1 and 4) and with 91.4 nM IolQ-his (lanes 2, 3, 5, and 6), and subjected to 12% polyacrylamide electrophoresis. Only in lanes 3 and 6, 1 mM myo-inositol was added. The positions of IolQ–DNA complex (C), free DNA (F), and negative control fragment (NC) are indicated by arrowheads.